

# Output-Only Modal Identification of a Cable-Stayed Bridge Using Wireless Monitoring Systems

Jian-Huang Weng<sup>1</sup>  
Chin-Hsiung Loh<sup>2</sup>  
Jerome P. Lynch<sup>3</sup>  
Kung-Chun Lu<sup>1</sup>  
Pei-Yang Lin<sup>4</sup>  
Yang Wang<sup>5</sup>

Submit to  
J. Engineering Structures

Submitted: April 26, 2006  
Revised: July 25, 2007

<sup>1</sup> Graduate Student, Department of Civil Engineering, National Taiwan University, Taipei, Taiwan.

<sup>2</sup> Professor, Department of Civil Engineering, National Taiwan University, Taipei, Taiwan. e-mail: [loh0220@ccms.ntu.edu.tw](mailto:loh0220@ccms.ntu.edu.tw) Tel: +886-2-2363-1799

<sup>3</sup> Assistant Professor, Department of Civil & Environmental Engineering, University of Michigan, Ann Arbor, USA

<sup>4</sup> Associate Research Fellow, National Center for Research on Earthquake Engineering, Taipei, Taiwan.

<sup>5</sup> Assistant Professor, School of Civil & Environmental Engineering, Georgia Institute of Technology, Atlanta, USA.

---

Corresponding author:

Prof. Chin-Hsiung Loh,

Department of Civil Engineering, National Taiwan University, Taipei, Taiwan

e-mail: [loh0220@ccms.ntu.edu.tw](mailto:loh0220@ccms.ntu.edu.tw) Fax: +886-2-2362-5044

## ABSTRACT

The objective of this paper is to present two modal identification methods that extract dynamic characteristics from output-only data sets collected by a low-cost and rapid-to-deploy wireless structural monitoring system installed upon a long-span cable-stayed bridge. Specifically, an extensive program of full-scale ambient vibration testing has been conducted to measure the dynamic response of the 240 meter Gi-Lu cable-stayed bridge located in Nantou County, Taiwan. Two different output-only identification methods are used to analyze the set of ambient vibration data: the stochastic subspace identification method (SSI) and the frequency domain decomposition method (FDD). A total of 10 modal frequencies and their associated mode shapes are identified from the dynamic interaction between the bridge's cables and deck vibrations within the frequency range of 0 to 7 Hz. The majority of the modal frequencies observed from recording cable vibrations are also found to be associated with the deck vibrations, implying considerable interaction between the deck and cables.

**Keywords:** Frequency domain decomposition, stochastic subspace identification, wireless structural monitoring, cable-stayed bridge.

## INTRODUCTION

A major engineering challenge associated with cable-supported bridges is complete characterization of the dynamic response of the bridge when loaded by traffic, wind and earthquakes. Accurate analysis of both the aerodynamic stability and the earthquake response of cable-stayed bridges often requires knowledge of the structure's dynamic characteristics, including modal frequencies, mode shapes and modal damping ratios. Conducting full-scale dynamic testing is regarded as one of the most reliable experimental methods available for assessing actual dynamic properties of these complex bridge structures [1]. Such tests serve to complement and enhance the development of analytical techniques and models that are integral to analysis of the structure over its operational life. During the past two decades, many researchers have conducted full-scale dynamic tests on suspension bridges including forced-vibration testing; however, there is comparatively less information available on full-scale dynamic testing of cable-stayed bridges. Typical examples of full-scale dynamic tests on bridges are provided in the references [1-4].

A simpler method for determination of the dynamic characteristics of structures is through the use of ambient vibration measurements. In output-only characterization, the ambient response of a structure is recorded during ambient influence (*i.e.* without artificial excitation) by means of highly-sensitive velocity or acceleration sensing transducers. The concurrent development of novel sensing technologies (*e.g.*, MEMS sensors, wireless sensors) and high-speed computing and communication technologies currently allow the engineering community to measure and evaluate ambient structural vibrations quickly and accurately. For example, wireless sensors represent an integration of novel sensing transducers with computational and wireless communication elements. Officials responsible for ensuring the long-term performance and safety of bridges depend upon empirically derived vibration characteristics to update analytical bridge models so that the chronological change of bridge load-bearing capacity can be tracked. As such, bridge officials direly need an economical

means of rapidly deploying sensors on a bridge to collect ambient response data from which modal information can be extracted; wireless sensors represent a transformative technology that uniquely meets these needs.

The use of wireless communications in lieu of wires within a structural monitoring system was initially proposed by Straser and Kiremidjian [5] as a means of reducing installation costs in large-scale civil structures. In addition, their work illustrated the freedom a wireless system infrastructure provides including rapid and reconfigurable installations. Recently, Lynch *et al.* has extended their work to include computational microcontrollers in the hardware design of wireless sensors so that various system identification and damage detection algorithms can be embedded for local execution by the sensor [6-8]. To date, a handful of bridges and buildings have been instrumented with wireless monitoring systems including the Alamosa Canyon Bridge (New Mexico), Geumdang Bridge (Korea), WuYuan Bridge (China), Voigt Bridge (California) and a historic theater in Detroit, Michigan [9]. These extensive field studies attest to the accuracy and reliability of wireless sensors in traditional structural monitoring applications.

The purpose of this study is to employ a rapid-to-deploy wireless structural monitoring system prototyped by Wang, *et al.* [10] for monitoring long-span bridges during ambient excitation conditions. Towards this end, this study will focus on the experimental determination of the dynamic properties of the newly retrofitted Gi-Lu cable-stayed bridge (Nantou County, Taiwan) using ambient vibration responses recorded by a wireless structural monitoring system. The wireless monitoring system consists of a distributed network of wireless sensors in direct communication with a high-performance data repository where data is stored and analyzed. To extract the bridge modal characteristics, both the frequency domain decomposition (FDD) and stochastic subspace identification (SSI) methods were embedded in the central repository to autonomously identify the dynamic properties of the bridge. The paper concludes with a discussion on the results obtained using the wireless

monitoring system, including observation of the interaction between cable and deck vibrations.

### **AMBIENT VIBRATION MEASUREMENTS**

The cable-stayed bridge selected for this study is the Gi-Lu Bridge, located in Nantou County, Taiwan. This bridge is a modern pre-stressed concrete cable-stayed bridge which crosses the Juosheui River. The bridge has a single pylon (with a 58 meter height above the deck) and two rows of harped cables (68 cables in total) on each side. The bridge deck consists of a box girder section 2.75 m deep and 24 m wide and is rigidly connected to the pylon; the deck spans 120 m on each side of the pylon. On September 21, 1999, during the final construction stages of the Gi-Lu Bridge, a significant earthquake (Chi-Chi Earthquake) with  $M_L = 7.3$  struck the central part of Taiwan. Only three kilometers away from the epicenter, Gi-Lu Bridge was subjected to very strong ground motions resulting in the damage of several of the bridge's critical structural elements. Reconstruction work undertaken to repair the bridge damage was completed at the end of 2004. At that time, the bridge owner elected to develop an experimentally-calibrated finite element model of the bridge so that bridge safety could be verified over the bridge operational lifespan. To accurately calibrate the model, an ambient vibration survey was conducted to extract the modal characteristics of the bridge. Subsequent model updating was done to minimize the difference between the modal characteristics (*e.g.* modal frequencies and mode shapes) of the model and those experimentally found.

***Instrumentation and data acquisition:*** To ensure a quick and low-cost means of collecting the dynamic response of the Gi-Lu bridge under ambient excitation conditions, a low-cost wireless monitoring system is used. The instrumentation installed in the bridge consisted of the following components: (1) *Wireless sensors:* twelve wireless sensors each containing a four-channel sensor interface with high-resolution analog-to-digital conversion

are used; (2) *Transducers*: interfaced to each wireless sensor node is a highly sensitive Tokyo Sokushin VSE-15 velocity meter whose sensitivity constant is 0.25Volt/kine (where 1 kine is equal to 1 cm/s); (3) *Data repository computer*: one high-performance laptop computer with a wireless modem serves as the core of the system responsible for triggering the system, archiving recorded response data, and autonomously extracting the bridge modal characteristics.

Due to the limited number of sensing nodes available (only 12 wireless sensor-velocity meter pairs), the wireless monitoring system is reconfigured during testing to achieve three different test configurations: (1) *Test 1*: Ten wireless sensor-velocity meter pairs are installed along the bridge deck to record its vertical vibration at locations denoted as V01 through V10 as shown in **Fig. 1a**; (2) *Test 2*: The ten wireless sensor-velocity meter pairs used during Test 1 are reoriented to record the deck's transverse vibration (denoted as H01 through H10 in **Fig. 1a**); (3) *Test 3*: All twelve wireless sensors are installed on one side of the bridge to simultaneously record the cables and deck vibrations at sensor location T01 through T12 (**Fig. 1b**). Data was sampled at 100 points per second on each channel to provide good waveform definition. The analog voltage output of the velocity meter was converted to a digital signal with 16-bit resolution by each wireless sensor. The synchronized time-histories collected by the wireless monitoring system were wirelessly broadcasted to the high-performance laptop computer serving as the monitoring system's sole data repository.

**Wireless sensors for structural monitoring:** A core element of this study was to assess the capabilities of a low-cost wireless structural monitoring system to rapidly collect the dynamic responses of a large-scale civil infrastructure system. A network of wireless sensing units, developed by Wang *et al.* [10] were installed upon the Gi-Lu Bridge in lieu of a traditional tethered structural monitoring system which are known to suffer from high-costs and laborious installations. The design of the wireless sensing unit is optimized for structural monitoring applications and includes three major subsystems: the sensing interface, the

computational core, and the wireless communication system. The sensing interface is responsible for converting analog sensor outputs spanning from 0 to 5V on four independent channels into 16-bit digital formats. Any sensing transducer can be interfaced to the wireless sensing unit with accelerometers, strain gages, displacement transducers and velocity meters all previously interfaced. The digital data is then transferred to the computational core by a high-speed serial peripheral interface (SPI) port. Abundant external memory (128 kB) is associated with the computational core for local data storage (up to 64,000 sensor data points can be stored at one time) and analysis. For reliable communication on the wireless channel, the Maxstream XStream wireless modem operating on the 2.4 GHz wireless band is selected. The outdoor communication range of the modem is up to 300 m line-of-sight which is sufficient for most large-scale civil structures. To enhance the range and reliability of communication in this study, directional antennas (D-link) were attached to each sensing unit to concentrate the energy associated with the wireless transmission in a concentrated beam pointed towards the central data repository. In summary, the hardware profile of the wireless sensing unit used in this study is presented in *Fig. 2*.

Embedded within each wireless sensing unit's computational core is software that automates operation in the field. A core element of the embedded software is a reliable communication protocol for the transfer of data between wireless sensing units and the data repository [10]. The protocol also is responsible for ensure the independent clocks associated with each wireless sensor is accurately time synchronized with the centralized repository. To synchronize the system, a beacon signal is broadcast by the central data repository; upon receipt of the beacon signal, each wireless sensing unit resets its internal clock to zero and begins to collect sensor data. Upon completion of its data collection tasks, data is communicated one wireless sensing unit at a time to the repository. The repository is required to confirm receipt of the data; should confirmation not be received by a wireless sensing unit, it will continue to transmit its data until the data successfully logged by the

repository. This communication protocol has been shown capable of time synchronization within 5 ms and has been shown immune to data loss [9]. A detailed overview of the communication protocol used for time synchronization and reliable data transfer is presented in *Fig. 3*.

Prior to installation in the field environment, extensive validation testing of the wireless communication channel are performed using the wireless prototype system installed upon a test structure at the National Center for Research on Earthquake Engineering (NCREE) in Taipei, Taiwan. The test structure consists of a full-scale three story steel frame subjected to different levels of earthquake excitation [11]. These tests revealed the wireless monitoring system to be: 1) easy to install, 2) accurate with wireless data identical to data collected from a tethered data acquisition system, 3) time synchronized within 5 ms, and 4) is highly reliable with no data loss in the wireless channel.

To successfully integrate the velocity meters with wireless sensing units, a signal converter is needed to modulate the output of the velocity meter (whose output spans  $\pm 10$  V) upon the allowable 0 to 5 V range of the sensing interface. The signal converter is designed as a stand-alone circuit that is placed between the velocity meter's output and the input of the wireless sensor. The converter circuitry mean shifts the velocity meter output (with 0 V mean) to 2.5 V without distortion to the signal. Provided ambient structural responses are being recorded, de-amplification of the velocity meter output is unnecessary for this study.

## **STOCHASTIC SUBSPACE IDENTIFICATION VERSUS FREQUENCY DOMAIN DECOMPOSITION**

By using wireless sensing units, the ambient vibration response of a bridge structure can be collected with ease and convenience. To extract modal information from the output-only data set generated by a wireless monitoring system, output-only system identification techniques can be applied. In this study, the stochastic subspace identification (SSI) method,

as originally presented by Van Overschee and De Moor [12], is adopted to identify a stochastic state space model of the Gi-Lu bridge using output-only measurements recorded by the wireless monitoring system. An extension of the original SSI method that does not require output covariance was proposed by Peeters and de Roeck [13] as the reference-based SSI method. Interested readers are referenced to [14]; a brief summary of the method is presented herein:

**Stochastic Subspace Identification:** Consider a discrete-time stochastic state-space model:

$$\begin{aligned} x_{k+1}^s &= Ax_k^s + w_k \\ y_k^s &= Cx_k^s + v_k \end{aligned} \quad (1)$$

where the superscript “s” denoting “stochastic” since the system is assumed to be excited by a stochastic component (*i.e.* broad-band noise). The SSI method is used to identify the system matrices,  $A$  and  $C$ , from the system output measurements,  $y_k^s$  (*i.e.* ambient vibration measurements). **Fig. 4** presents the detail procedure for identification of the system matrix,  $A$ , by the SSI method:

**1. Using output measurement data, the Hankel matrix,  $Y^s$ , can be constructed:**

$$Y^s \equiv \begin{bmatrix} y_0^s & y_1^s & \cdots & y_{j-1}^s \\ y_1^s & y_2^s & \cdots & y_j^s \\ \cdots & \cdots & \cdots & \cdots \\ y_{i-1}^s & y_i^s & \cdots & y_{i+j-2}^s \\ y_i^s & y_{i+1}^s & \cdots & y_{i+j-1}^s \\ y_{i+1}^s & y_{i+2}^s & \cdots & y_{i+j}^s \\ \cdots & \cdots & \cdots & \cdots \\ y_{2i-1}^s & y_{2i}^s & \cdots & y_{2i+j-2}^s \end{bmatrix} \equiv \begin{bmatrix} Y_p^s \\ Y_f^s \end{bmatrix} \in \mathbb{R}^{2li \times j} \quad (2)$$

where  $i$  is a user-defined index and must be larger than the order,  $n$ , of the system. Since there are only  $l$  degrees-of-freedom measured, (in this study,  $l=10$  or  $12$  depending upon whether 10 or 12 measurement locations are used in the three test

setups), the output vector  $y_k^s$  must contain  $l$  rows and the matrix  $Y^s$  must contain  $2li$  rows. Here,  $j$  corresponds to the number of columns of the Hankel matrix. To ensure all of the  $r$  time samples of the output vector  $y_k^s$  populate the Hankel matrix, the number  $j$  can be equal to  $r-2i+1$ . According to the expression of Eq. (2), the Hankel matrix is divided into the past,  $Y_p^s \in \mathbb{R}^{li \times j}$ , and the future,  $Y_f^s \in \mathbb{R}^{li \times j}$ , parts. For the reference-based stochastic subspace identification method, the Hankel matrix plays a critically important role in the SSI algorithm.

## 2. Row Space Projections:

The orthogonal projection of the row space of the matrix  $Y_f^s \in \mathbb{R}^{li \times j}$  on the row space of the matrix  $Y_p^s \in \mathbb{R}^{li \times j}$  is defined as  $Y_f^s / Y_p^s$  which can be calculated by the following formula:

$$Y_f^s / Y_p^s \equiv Y_f^s Y_p^{sT} \left( Y_p^s Y_p^{sT} \right)^\dagger Y_p^s = O_i^s \in \mathbb{R}^{li \times j} \quad (3)$$

where “/” denotes the projection operator,  $T$  denotes the transpose operator and  $\dagger$  denotes the pseudo-inverse operator. The projection operator can also be computed quickly by using QR-decomposition [13]. QR-decomposition of the block Hankel matrix ( $H=RQ^T$ ) results in a reduction of the computational complexity and memory requirements of the SSI implementation by projecting the row space of future outputs into the row space of the past reference outputs. Orthogonal projection relates the Hankel matrix to the observability matrix; hence, the observability matrix can be estimated by factoring the orthogonal projection of the Hankel matrix.

## 3. Singular value decomposition (SVD) of the orthogonal projection:

In linear algebra, SVD is an important factorization tool used for rectangular real or complex matrices. SVD is used to decompose the orthogonal projection of the Hankel matrix:

$$O_i^s = USV^T = (U_1 \quad U_2) \begin{pmatrix} S_1 & 0 \\ 0 & S_2 \end{pmatrix} \begin{pmatrix} V_1^T \\ V_2^T \end{pmatrix} \approx U_1 S_1 V_1^T \quad (4)$$

The matrix  $U \in \mathbb{R}^{li \times li}$  contains a set of orthonormal ‘‘output’’ basis vector directions for  $O_i^s$  while  $V \in \mathbb{R}^{j \times j}$  contains a set of orthonormal ‘‘input’’ basis vector directions for  $O_i^s$ . The matrix  $S \in \mathbb{R}^{li \times j}$  contains singular values of the decomposition along its diagonal; here,  $S$  is block separated into two parts  $S_1$  and  $S_2$ . The smallest singular values in the matrix  $S$  are grouped as  $S_2 \in \mathbb{R}^{(li-n) \times (j-n)}$  and are neglected. In contrast, the largest set of singular values,  $S_1$ , dominate the system and provide a means of assessing the system order. The order,  $n$ , is the number of dominant singular values where  $S_1 \in \mathbb{R}^{n \times n}$ . Thus a reduced version of the SVD is described by the matrices  $U_1 \in \mathbb{R}^{li \times n}$ ,  $S_1 \in \mathbb{R}^{n \times n}$  and  $V_1 \in \mathbb{R}^{j \times n}$ . A reduced SVD helps to catch the principle components of the system and reduce noise effects.

**4. Calculate the extended observability matrix,  $\Gamma_i$ :**

$$\Gamma_i = U_1 S_1^{1/2} \quad (5)$$

Since the dimension of  $\Gamma_i$  in Eq. (5) is  $li \times n$ , it can be extracted from the reduced order SVD of the orthogonal projection as described above. The extended observability matrix  $\Gamma_i$  is defined as:

$$\Gamma_i \equiv \begin{bmatrix} C \\ CA \\ CA^2 \\ \dots \\ CA^{i-1} \end{bmatrix} \in \mathbb{R}^{li \times n} \quad (6)$$

which contains information on the system matrix,  $A$ .

**5. Calculate the system parameter matrices  $A$  and  $C$  from  $\Gamma_i$ :**

$$A = \underline{\Gamma}_i^\dagger \bar{\Gamma}_i \quad (7)$$

where  $\underline{\Gamma}_i \in \mathbb{R}^{(i-1) \times n}$  denotes  $\Gamma_i$  without the last  $l$  rows and  $\bar{\Gamma}_i \in \mathbb{R}^{l(i-1) \times n}$  denotes  $\Gamma_i$  without the first  $l$  rows. The matrix  $C$  can be determined from the first  $l$  rows of  $\Gamma_i$  as shown in Eq. (6).

**6. Calculate the eigenvalues,  $\lambda_N$ , and eigenvectors,  $\phi_{\lambda_N} \in \mathbb{R}^{n \times 1}$ , of  $A$ :**

$$\det(A - \lambda_N I) = 0, \quad (A - \lambda_N I)\phi_{\lambda_N} = 0 \quad (8)$$

It should be noted that the eigenvalues of  $A$  occur in complex conjugated pairs and the subscript “ $N$ ” denotes the number of these pairs.

**7. Determine the frequency  $\omega_N$  and damping coefficient  $\xi_N$  from  $\lambda_N$ :**

$$\omega_N = \frac{a_N}{2\pi\Delta t} \text{ (rad/s)}, \quad \xi_N = \frac{|b_N|}{\sqrt{a_N^2 + b_N^2}} \quad (9)$$

where

$$a_N = \left| \arctan \left( \frac{\text{Im}(\lambda_N)}{\text{Re}(\lambda_N)} \right) \right|, \quad b_N = \ln(|\lambda_N|) \quad (10)$$

**8. Determine mode shapes  $\Phi_N$  (with corresponding frequency  $\omega_N$ ) from  $C$  and  $\phi_{\lambda_N}$ :**

$$\Phi_N = C\phi_N \quad (11)$$

The elements in the vector,  $\Phi_N$ , are always complex numbers in practice. It can be imagined that the absolute value of the complex number is interpreted as the amplitude and the argument as the phase of a sine wave at a given frequency,  $\omega_N$ .

In the SSI method, first, the output data collected from the ambient vibration survey is arranged to form the Hankel matrix. Second, the projection theorem is introduced to establish the relation between the extended observability matrix and the matrix corresponding to the orthogonal projection. Finally, the SVD algorithm is used to determine the system matrix,  $A$ , from which the dynamic characteristics ( $\Phi_N, \omega_N, \xi_N$ ) of the system can be identified.

**Frequency Domain Decomposition (FDD) method:** A second modal estimation method is adopted in this study termed the frequency domain decomposition (FDD) method [15]. In this identification method, the first step is to estimate the power spectral density (PSD) matrix from the measurements and then decomposed at  $\omega = \omega_i$  by taking the SVD of the matrix:

$$\hat{G}_{yy}(j\omega_i) = U_i S_i U_i^T \quad (12)$$

where the matrix  $U_i = [u_{i1}, u_{i2}, \dots, u_{im}]$  is a matrix holding the singular vectors  $u_{ij}$ , and  $S_i$  is a diagonal matrix holding the scalar singular values  $s_{ij}$ . If only the  $k^{\text{th}}$  mode is present at the selected frequency,  $\omega_i$ , then there will be only one singular value in Eq. (12). Thus, the first singular vector  $u_{i1}$  would then serve as an estimate of the  $k^{\text{th}}$  mode shape,  $\hat{\phi} = u_{i1}$ . To implement the FDD method, some prior knowledge of the modal frequencies is required; traditional peak-picking methods can be adopted using the frequency response function of the system calculated for each system output. An advantage of the FDD method is that if two modes are closely spaced and can be identified previously (*e.g.* using the aforementioned SSI method), they can be identified based upon multiple singular values present at a selected frequency.

### **ANALYSIS OF BRIDGE AMBIENT VIBRATION DATA: DYNAMIC PROPERTIES OF THE DECK AND CABLES**

Using the reference-based stochastic subspace identification method described above, the dynamic characteristics of the Gi-Lu cable-stayed bridge are accurately identified from the wireless sensor data collected during field study. Results obtained from the wireless monitoring system and application of the SSI method are highlighted below:

#### **1. Data analysis using all output measurements from the deck simultaneously:**

Integral to implementation of the SSI method are two parameters that need to be determined *a priori*. The first is the number of block rows,  $i$ , and the second is the appropriate order,  $n$ , of the system. Both parameters directly influence the structure of the stochastic output Hankel matrix  $Y^s$  as it is constructed from the output data sequences according to  $i$ ; a reduced version of the Hankel matrix obtained by SVD is also determined according to the order,  $n$ . The influence of both parameters on the corresponding system identification results can be explained by the number of block rows,  $i$ , affecting the precision of the SSI method while  $n$  corresponds to the number of structural modes contained by the SSI model. In this study, we start with determining  $n$  by giving a fixed value of  $i$  while  $j$  is varied. In other words, the number of data points,  $r$  (equal to  $2i + j - 1$ ), contained in the output vector,  $y_k^s$ , varies in tandem with the value of  $j$  selected.

For illustration, a simple case is used to demonstrate how the system order is determined. Consider the case where only the vertical response of the bridge deck is measured from the 10 wireless sensing units. **Fig. 5** plots the quantity of each singular value resulting from the decomposition of the projection of the past on the future outputs of the Hankel matrix as a function of the number of block columns  $j$ . It is clear that the singular values rapidly diminish with the singular values stabilizing to a small value at the 22<sup>th</sup> singular value ( $s_{22} = 0.0235$ ). As a result of this qualitative observation, the order of the system is determined as  $n = 22$ . With the system order determined, the analysis returns to determine the number of block rows  $i$  using a fixed number of sampled data points,  $r = 5000$ . To assess if a suitable number of block rows is selected, the sensitivity of the modal frequencies and damping coefficients are compared as a function of  $i$ . **Fig. 6** plots the identified modal frequency and damping coefficient of the first four modes as a function of  $i$ . The variability of the model frequencies looks small but the modal damping coefficients are uncertain and illegitimate when a small number  $i$  is used. This figure also proves the hypothesis that  $i$  is

closely related to the precision of SSI method. Considering the modal frequencies and damping coefficients determined for the vertical response of the bridge deck, the number of block rows is selected as 110 for this case ( $r = 5000$ ). Furthermore, it should be noticed that the system order  $n$  is directly linked to the number of modes contained in the SSI model. In general, the number of true structural modes identified will not exceed half the number of modes contained in the SSI model. As a result, it is important to note that selection of an unwarranted large system order without examination on regulation will increase the number of modes but the result in many unreliable “noise” modes.

*Fig. 7* shows typical velocity time histories recorded on the Gi-Lu bridge deck and cables during ambient excitation (recorded during Test 3). Using time history data collected during Test 1 and 3, the modal frequencies of the bridge determined by the high-performance data repository executing the reference-based SSI method are tabulated in *Table 1*. In addition, the first ten bridge deck mode shapes determined by the SSI method during Test 1 are shown in *Fig. 8a*. Using the FDD method (using the specific frequency identified from the SSI method), a second set of identified mode shapes of the bridge are determined and plotted on the same figure (*Fig. 8a*) for comparison. The estimated mode shapes of the bridge deck using both methods are consistent. Using the time history data collected during Test 2, the identified mode shapes of the bridge deck in the transverse direction are also shown in *Fig. 8b*. Again, excellent agreement between SSI- and FDD-derived mode shapes is evident.

## ***2. Data Analysis from the interaction between deck and cable vibration:***

The SSI method is also applied to the data collected during the Test 3 setup. The identified dominant frequencies from this data set are tabulated in *Table 1*. After data has been collected, Fourier analysis is applied on the same data set off-line. *Fig. 9a* and *Fig. 9b* plot the Fourier amplitude spectra of both the horizontal and vertical ambient vibration of the two instrumented bridge cables (R13 is a short cable and R27 is a long cable). From the

Fourier amplitude spectrum of cable vibration data, there are several dominant frequencies in the lower frequency range which belong to the deck vibration modes and not the cable itself. This can be better observed from *Fig. 8c* where the Fourier amplitude spectrum of the cable vibration data and the deck vibration data are plotted on the same graph. By comparing the identified dominant frequencies using the SSI and off-line Fourier methods, one can clearly observe that the close interaction between the deck and cable vibrations, particularly in the lower frequency range (0 – 2 Hz).

### ***3. Model updating of a finite element model of the Gi-Lu Bridge:***

Motivation of the use of a wireless monitoring system is its ability to be rapidly deployed by bridge owners for low-cost yet accurate assessment of bridge modal properties. Such properties are integral to updating finite element models used by engineers to assess the condition of the structure over its operational life. Toward this end, an analytical model of the Gi-Lu Bridge had been developed using a MATLAB- based computer program [16]. The code includes the use of traditional beam elements for the bridge structure and nonlinear beam elements to represent cables with sag and pre-tension forces. After updating the analytical model, the first calculated fundamental frequency of the bridge model is 0.5148Hz which corresponds to the deck's first vertical vibration mode. **Table 2** shows the comparison between the identified deck vibration frequencies using ambient vibration data collected during field study and the numerical results of the updated model. Excellent results are obtained with good agreement evident between the numerical model and the test data.

## **CONCLUSIONS**

The purpose of this paper is to conduct an ambient vibration survey of a long-span cable-stayed bridge and to develop a systematic method for the extraction of the dynamic characteristics of the bridge using data collected by a novel wireless monitoring system. The

following conclusions are drawn from the full-scale measurements made on the Gi-Lu Bridge:

1. The wireless sensing units were used in lieu of more costly tethered data acquisition systems. Less effort and man-power were required during the installation of the wireless monitoring system rendering it as ideally suited for rapid short-term field studies. Because the wireless communication range in the open field can reach up to 300 m, it was possible to successfully collect data from at least 10 sensors (in this study) simultaneously with a sampling rate of 100 Hz. During data collection, the wireless monitoring system experienced no data loss as a result of a highly robust communication protocol.
2. The measurement of structural response to ambient levels of wind and traffic has proved to be an effective means of identifying the dynamic properties of a full-scale cable-stayed bridge. The dynamic properties that have been identified from these measured responses are modal frequencies, mode shapes and estimates of modal damping ratios.
3. To autonomously extract the dynamic characteristics of the bridge from structural response time histories, two different approaches were used: the SSI method and the FDD method. Detail description on the time domain dynamic characteristic identification using multiple output identification (SSI method) can extract the mode shape directly. The SSI method can provide a good estimation of the number of modes observed in the structure based on singular values of the Hankel matrix projection. On the other hand, the FDD method can only be applied in the frequency domain if the dominant frequencies are determined *a priori*.
4. The results of this test have provided conclusive evidence of the complex dynamic behavior of the bridge. The dynamic response of the cable-stayed bridge is characterized by the presence of many closely spaced, coupled modes. The analytical results of this cable-stayed bridge had been studied before [16]. For most modes, the analytical and the experimental modal frequencies and mode shapes compare quite well. Based on the analysis of ambient vibration data, it is evident that the vertical vibration of the bridge deck is tightly coupled

with the cable vibrations within the frequency range of 0 to 3 Hz.

5. In order to identify the coupling effect between the bridge deck and cables, different instrumentation architectures are adopted (specifically, Test 1, Test 2 and Test 3 in this study). The stochastic subspace identification method provides a very effective way to identify the mode shapes of the structure through the spatially distributed sensors. It can compress the data while preserving vibration information and also eliminate uncorrelated noise. Through a comparison of the results corresponding to different test setups, separation of dominant frequencies between the bridge deck and cable can be easily identified. As for the damping ratio estimation, the first vibration mode of the deck had a damping ration of 2.5% on average (depends upon the different sensor locations); the damping values for higher modes are less than 1.0%. More detail study on the estimation of accurate damping ratios is needed in future research.

### **ACKNOWLEDGEMENTS**

The authors wish to express their thanks to Central Weather Bureau (MOTC-CWB-94-E-13) as well as National Science Council (NSC95-2221-E-002-311) on the support of this research. The authors wish to thanks Mr. Chia-Ming Chang for his assistance to provide the analytical result of the bridge which is referenced in companion papers.

### **REFERENCES**

- [1] Ko JM, Sun ZG, Ni YQ. Multi-stage identification scheme for detecting damage in cable-stayed Kap Shui Mun Bridge. *Engineering Structures* 2002; 24(7):857-868.
- [2] Ozkan E, Main J, Jones NP. Long-term measurements on a cable-stayed bridge. IMAC-paper 2001.
- [3] He X, Moaveni B, Conte JP, Elgamal A, Masri SF, Caffrey JP et al. System Identification of New Carquinez Bridge Using Ambient Vibration Data. *Proc. of Int. Conf. on*

Experimental Vibration Analysis for Civil Engineering Structures, Bordeaux, France, Oct., 2005,26-28.

- [4] Wenzel H, Pichler D. Ambient Vibration Monitoring, John Wiley & Sons, Ltd, 2005.
- [5] Straser EG, Kiremidjian AS. A modular, wireless damage monitoring system for structure, Report No.128, John A. Blume Earthquake Center, CE Department, Stanford University, Stanford CA., 1998.
- [6] Lynch JP, Sundararajan A, Law KH, Kiremidjian AS, Carryer E. Embedding damage detection algorithms in a wireless sensing unit for operational power efficiency. *Smart Materials and Structures* 2004; 13(4): 800-810.
- [7] Lynch JP, Sundararajan A, Law KH, Kiremidjian AS, Kenny TW, Carryer E. Embedment of structural monitoring algorithms in a wireless sensing unit. *Structural Engineering and Mechanics* 2003; 15(3): 285-297.
- [8] Lynch JP. An overview of wireless structural health monitoring for civil structures. *Philosophical Transactions of the Royal Society of London. Series A, Mathematical and Physical Sciences* 2007; 365(1851): 345-372.
- [9] Lynch JP, Wang Y, Loh K, Yi JH, Yun CB. Performance Monitoring of the Geumdang Bridge using a Dense Network of High-Resolution Wireless Sensors, *Smart Materials and Structures* 2006; 15(6): 1561-1575.
- [10] Wang Y, Lynch JP, Law KH. A Wireless Structural Health Monitoring System with Multithreaded Sensing Devices: Design and Validation, *Structure and Infrastructure Engineering* 2007; 3(2): 103-120.
- [11] Lynch JP, Wang Y, Lu KC, Hou TC, Loh CH. Post-seismic Damage Assessment of Steel Structures Instrumented with Self-Interrogating Wireless Sensors, Proc. of 8-th US National Conf. on Earthquake Engineering, paper No.1390, San Francisco, US, April, 2006.
- [12] Van Overschee P, De Moor B. Subspace algorithm for the stochastic identification

problem. *Automatica* 1993; 29(3): 649-660.

- [13] Peeters B, De Roeck G. Reference-Based Stochastic Subspace Identification for Output-Only Modal Analysis. *Mechanical systems and Signal Processing* 1999; 13(6): 855-878.
- [14] Van Overschee P, De Moor B. *Subspace Identification for Linear System: Theory-Implementation-Applications*, Dordrecht, Netherlands: Kluwer Academic Publishers, 1996.
- [15] Brincker R, Zhang L, Anderson P. Modal identification of output-only systems using frequency domain decomposition. *Smart Materials and Structures* 2001; 10(3): 441-445.
- [16] Loh CH, Chang CM. MATLAB-based seismic response control of a cable-stayed bridge: cable vibration. *Structural Control and Health Monitoring* 2007; 14(1): 109-143.

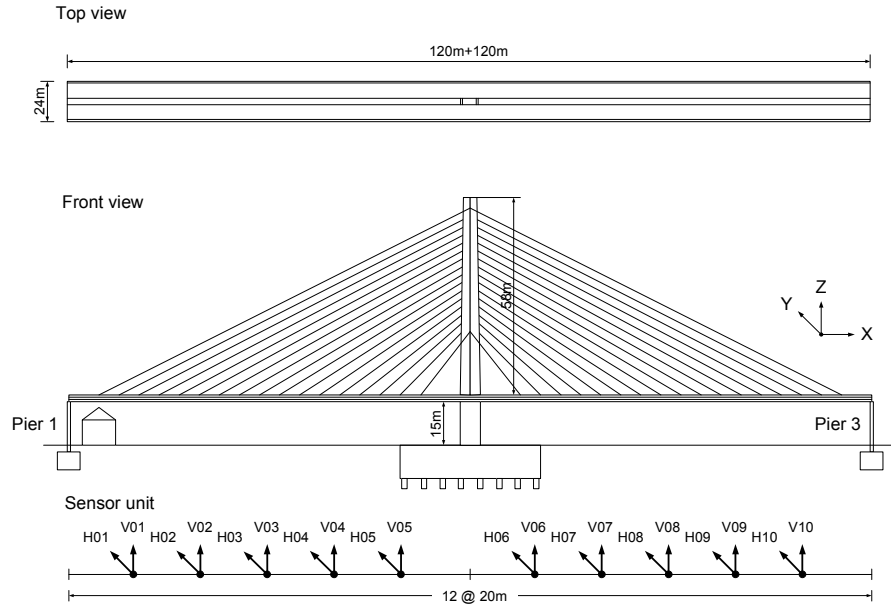


**Figure 1a:** Front view and top view of the Gi-Lu cable-stayed bridge. Locations of velocity meter-wireless sensor pairs installed (in vertical and transverse directions, for Test 1 and Test 2, respectively) along the bridge deck for the ambient vibration survey.

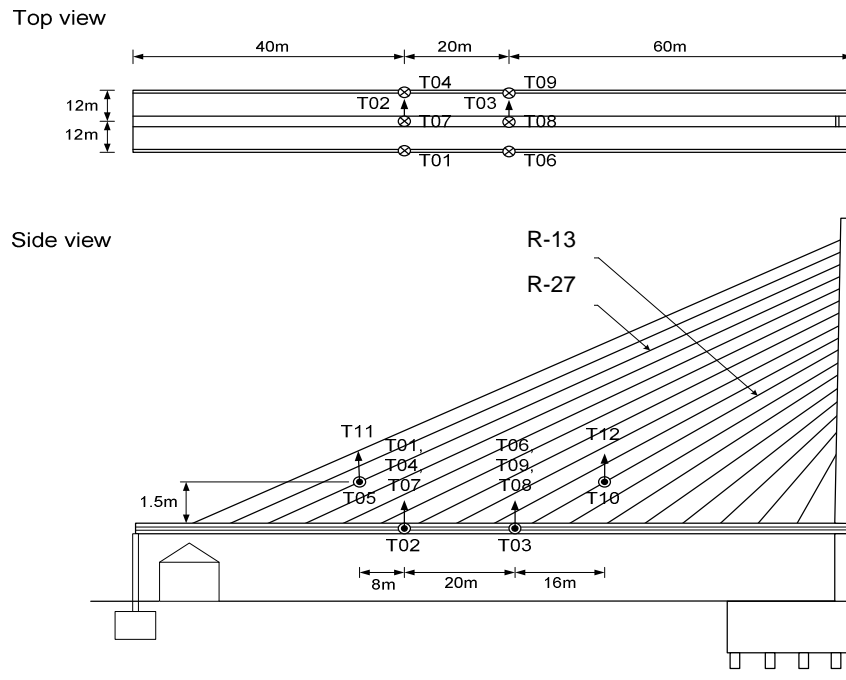


**Figure 1b:** Installation location of the wireless sensors during Test 3; velocity meters are installed to record the ambient response of the deck and cables simultaneously.

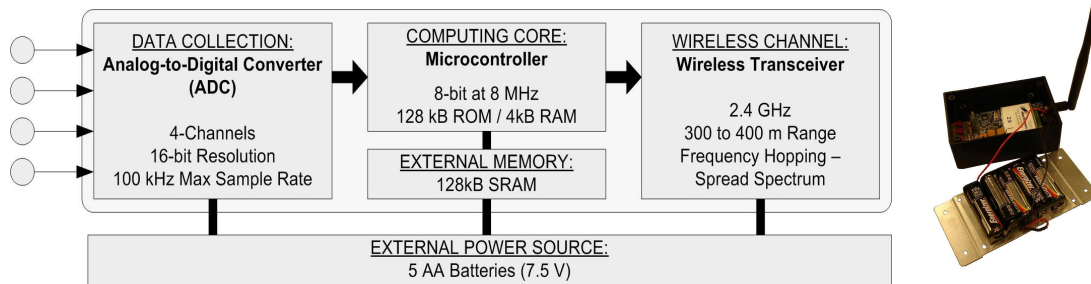


**Figure 2:** Overview of the hardware design of a wireless sensor prototype for structural monitoring applications [10].

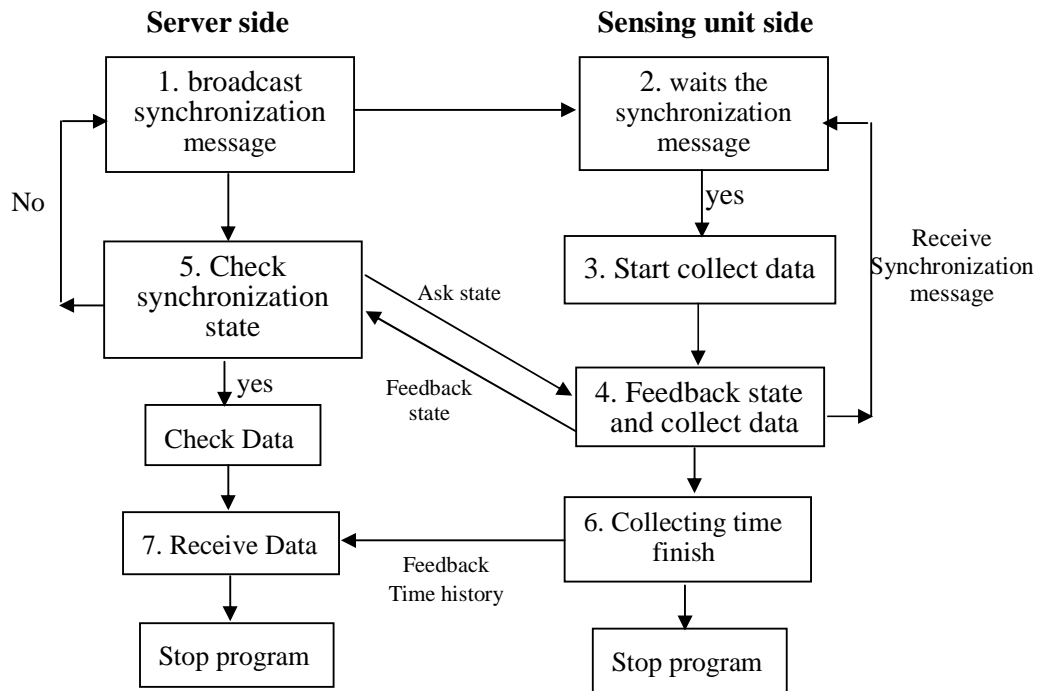


**Figure 3:** State diagram detailing time-synchronized communication between wireless sensing units and the data server.

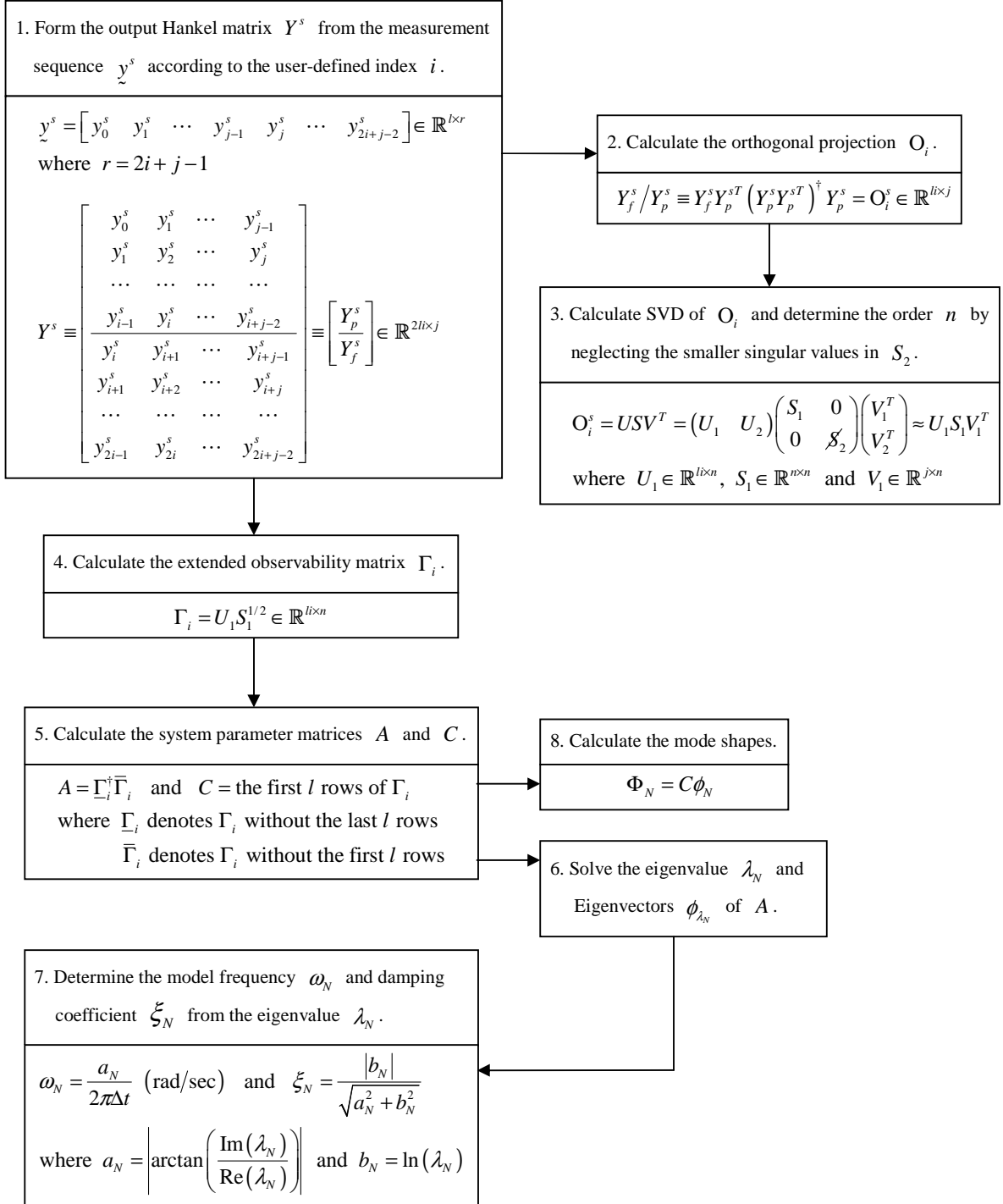


**Figure 4:** Flow chart of Stochastic Subspace Identification (SSI) technique.

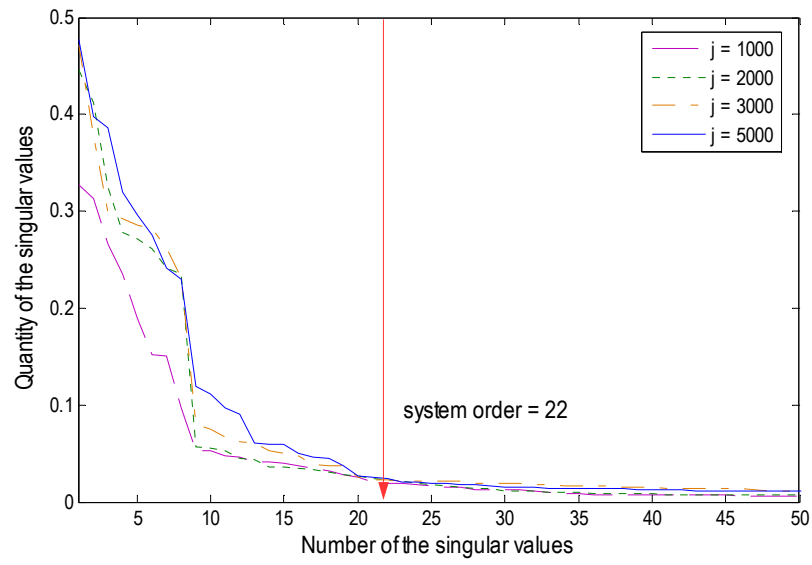
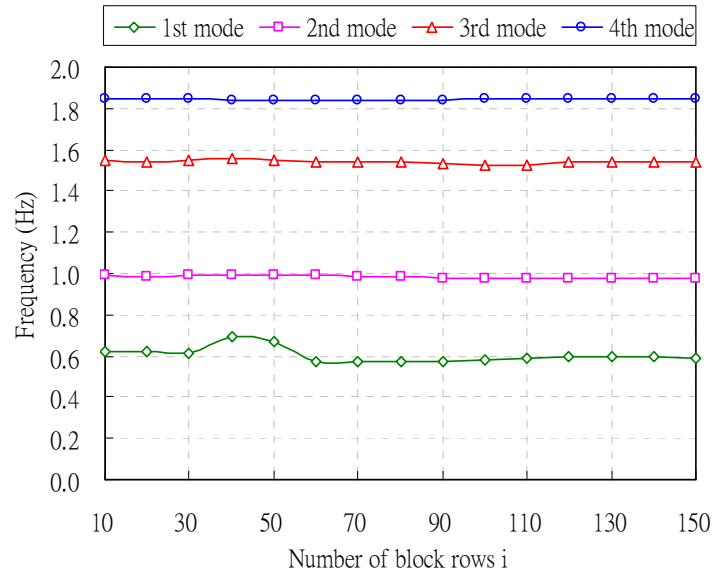


**Figure 5:** Plot of the singular value quantity as a function of the singular value index.

(a)



(b)

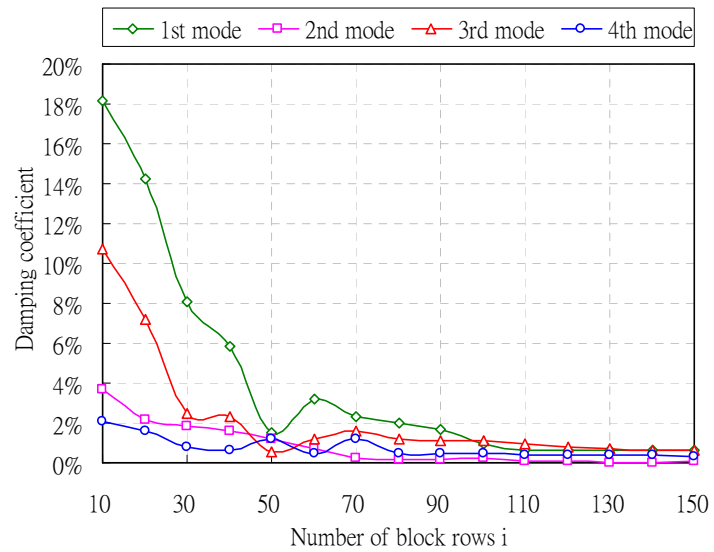


**Figure 6:** Relationship between the estimated modal parameters, natural frequency (a) and damping ratio (b), and the number of block rows “ $i$ ”. The sensitivity of the modal frequencies (a) and damping coefficients (b) can be identified with respect to “ $i$ ”.

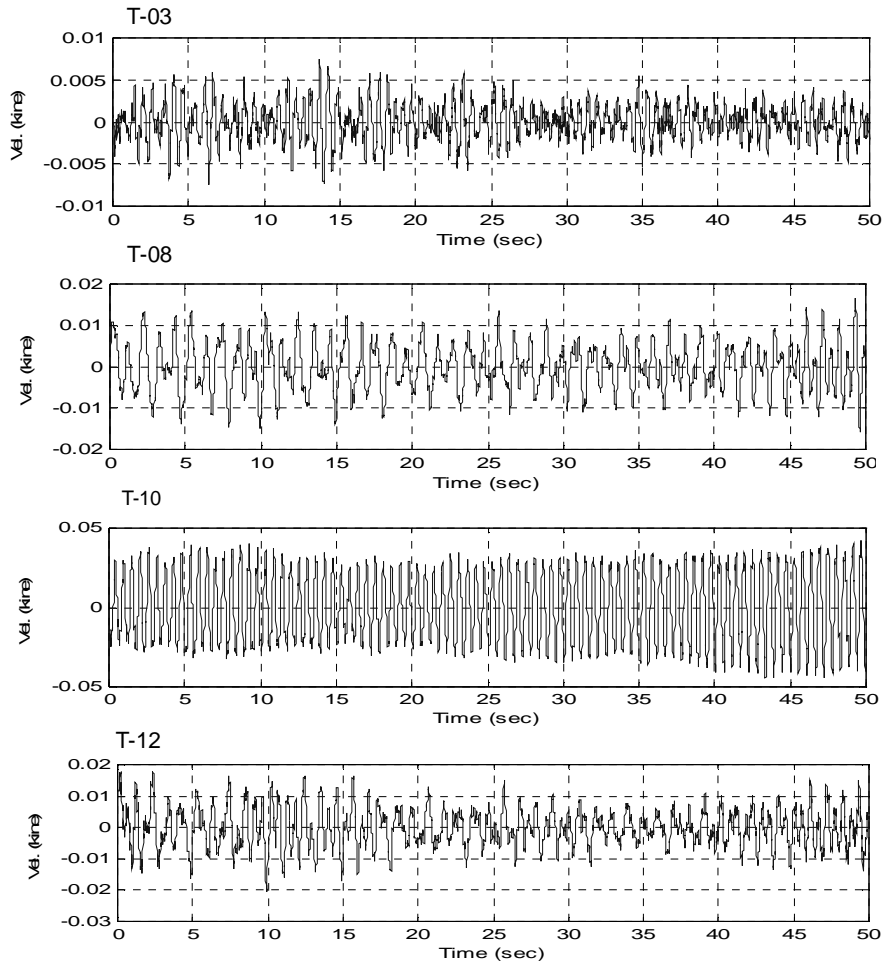


**Figure 7:** Recorded ambient vibration signals (velocity) at sensor location T03, T08, T10 and T12 (Fig.1b)( during Test-3.

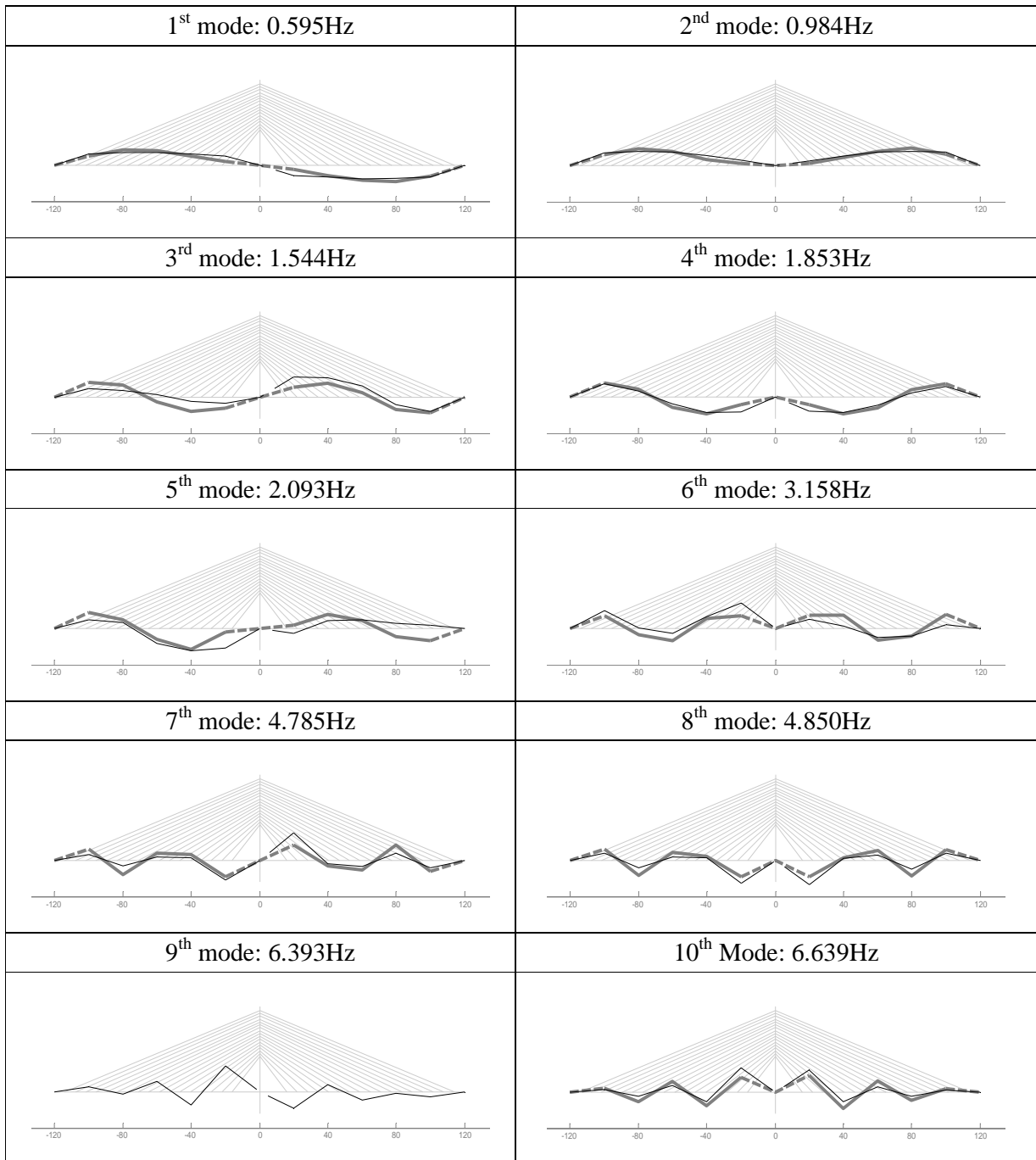
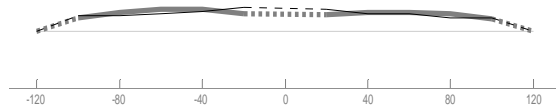
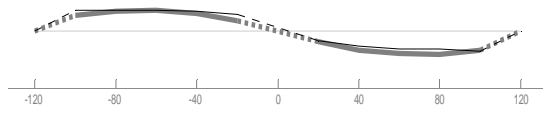


**Figure 8a:** Comparison of the identified bridge deck vertical mode shapes by using the reference-based stochastic subspace identification and frequency domain decomposition methods.

1<sup>st</sup> Mode : 1.449Hz



2<sup>nd</sup> mode : 1.552Hz



3<sup>rd</sup> mode : 2.917Hz

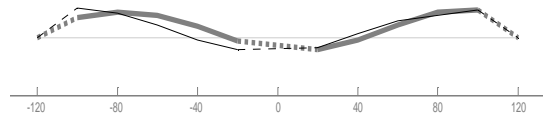


**Figure 8b:** Comparison of the identified bridge deck mode shapes in the transverse direction by using the reference-based stochastic subspace identification and frequency domain decomposition methods.

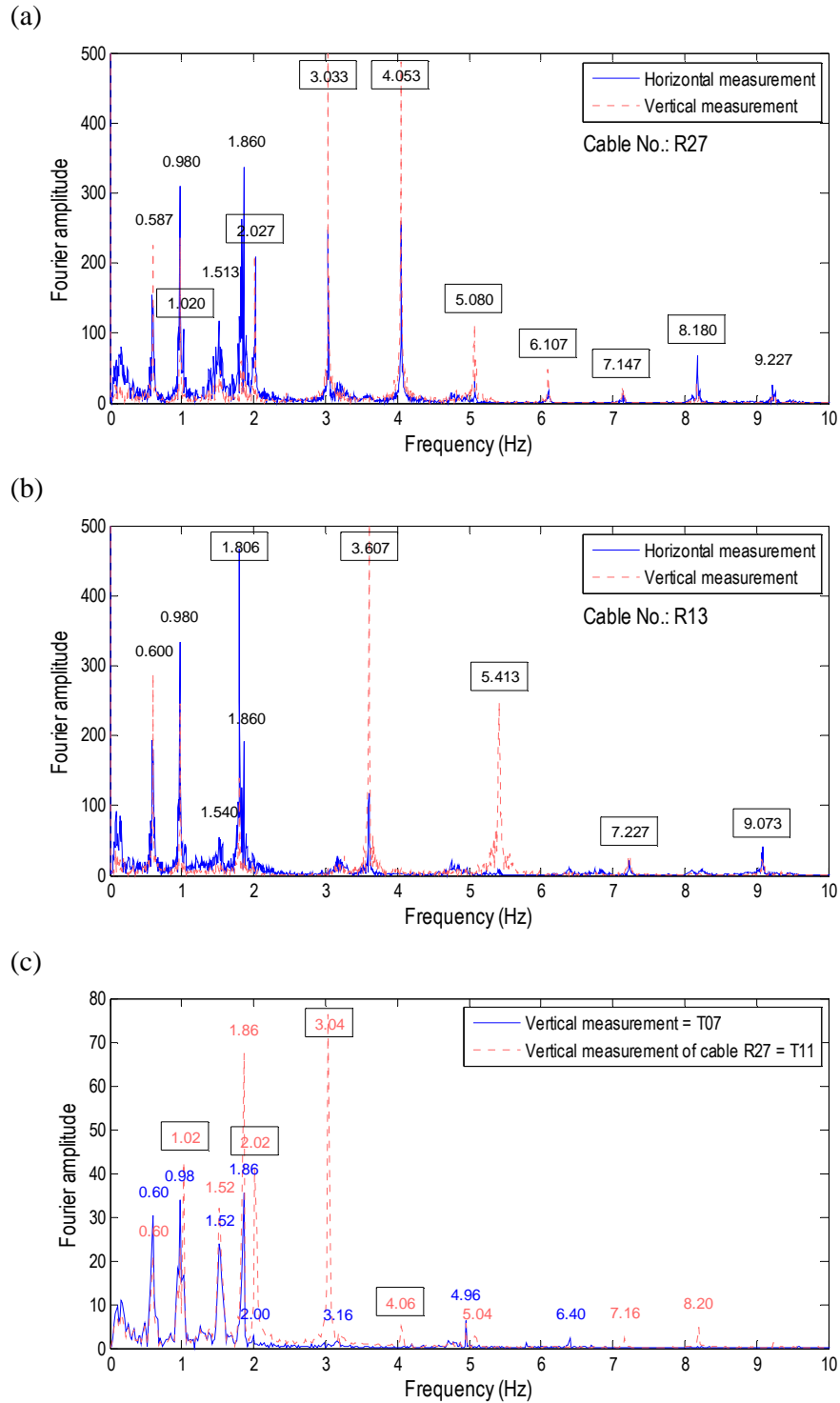


**Figure 9:** Fourier amplitude spectrum of cable vertical and horizontal vibration data (Fig. 9a for cable R-27 and Fig. 9b for cable R-13). The number in the box is the identified dominant frequency of cable. Comparison on the Fourier amplitude spectrum of cable vibration and deck vertical vibration is shown in Fig.9c.

**Table 1:** Identified natural frequencies from Test-1 and Test-3 using SSI method. The dominant frequencies of cables R-13 and R-27 are also shown.

Test-1* Freq. (Hz)	Test-3* Freq. (Hz)	R-13 Cable** Dominant freq. (Hz)	R-27 Cable** Dominant freq. (Hz)	Note
0.595	0.600	0.600	0.578	1 <sup>st</sup> vertical model freq.
0.985	0.975	0.980	0.980	2 <sup>nd</sup> vertical model freq.
	1.019	/	1.020	R-27 Cable 1 <sup>st</sup> vibration freq.
	1.462	/		Torsion model freq.
1.544	1.539	1.540	1.540	3 <sup>rd</sup> vertical model freq.
	1.809	1.806		R-13 cable 1 <sup>st</sup> vibration freq.
1.853	1.871	1.860	1.860	4 <sup>th</sup> vertical model freq.
2.093	2.029	/	2.027	5 <sup>th</sup> vertical model freq. R-27 cable 2 <sup>nd</sup> model freq.
3.158	/	3.607	3.033	/
4.785	/	5.413	4.053	/
4.850	/	7.227	5.080	/
6.639				

\*: identified using stochastic subspace identification method,

\*\* : identified directly from Fourier analysis of measurements,

**Table 2:** Comparison between the identified deck vibration natural frequencies and numerical model frequencies from simulation.

Analytical Mode	1 <sup>st</sup> Mode	31 <sup>th</sup> mode	64 <sup>th</sup> mode	102 <sup>th</sup> mode	115 <sup>th</sup> mode
Model frequency	0.5148 Hz	1.0505 Hz	1.4457 Hz	1.8940 Hz	2.0378 Hz
Identified Mode (from Ambient Data)	1 <sup>st</sup> Mode	2 <sup>nd</sup> Mode	3 <sup>rd</sup> Mode	4 <sup>st</sup> Mode	5 <sup>th</sup> mode
Model frequency	0.595 Hz	0.985 Hz	1.544 Hz	1.853 Hz	2.093 Hz